

Novel Antibacterial Composite of Coal/LLDPE Loaded with Silver Ions

Anning Zhou, Zhanjiang Yu

Department of Chemistry and Chemical Engineering, Xi'an University of Science and Technology, Xi'an 710054, People's Republic of China

Received 8 April 2006; accepted 29 June 2006

DOI 10.1002/app.25044

Published online 25 April 2007 in Wiley InterScience (www.interscience.wiley.com).

ABSTRACT: A novel antibacterial composite of coal/LLDPE (linear low density polyethylene) loaded with silver ions (ACCPE) was prepared by means of solid-liquid phase adsorption and extrusion. The composite was characterized by IR, XRD and SEM, and the mechanical, rheological, and Ag⁺-releasing, and antibacterial properties of the composite were investigated. We discover that the ACCPE shows favorable mechanical

properties, features a higher processability and antibacterial activity, and the coal and silver ion possess superimposed effect on antibacterial activity against *Escherichia coli*. © 2007 Wiley Periodicals, Inc. *J Appl Polym Sci* 105: 1559–1565, 2007

Key words: metal-polymer complexes; functionalization of polymers; composites; rheology; adsorption

INTRODUCTION

Bacteria such as *Escherichia coli* easily breed in an emitting pipe especially at jointed parts and in dripping holes due to long-term irrigation and contact with soil, and even the bacteria jam the dripping holes to the full. To solve this problem, we prepared the novel antibacterial material.

Silver has been known as a disinfectant for many years and is being used in many forms in the treatment of infectious diseases,^{1–3} and has a broad spectrum of antibacterial activity while exhibiting low toxicity toward mammalian cells. Ionic silver has the highest antibacterial activity among metal ions.^{4,5} Silver ions, even in a very low concentration, are effective against bacteria in water systems.^{6,7} Furthermore, ionic silver possesses novelty being a long-lasting biocide.⁸

Coal is a natural porous organic mineral material with extended surface area, high adsorption amount and rate, specific surface reactivity, and exhibits a strong affinity and sorption for Ag⁺. At the same time, coal itself features strong antibacterial activity against bacteria.⁹ These macroscopically chemical or physical properties of coal are related to coal molecular structure and could be explained through a typ-

ical Shinn model of coal molecular structure¹⁰ (Fig. 1).

Our key work is to adequately combine coal (with low cost and antibacterial activity) with silver (with long-lasting biocide and broad spectrum of antibacterial activity) to develop a novel antibacterial composite, which can provide antibacterial activity to resins or plastics by mixing.

MATERIALS AND METHODS

Materials

Shenfu coal (Shenfu coalfield, Shaanxi, China) was used as an adsorbent for Ag⁺ and a filling material for polymer of LLDPE 7042, and was grounded to $D_{97} \leq 12 \mu\text{m}$ particle size using a planetary ball miller (Nanjing University, China, QM-BP). Table I lists proximate and ultimate analysis of the raw Shenfu coal mentioned earlier. The polymer of LLDPE 7042 was obtained from SINOPEC Yanshan Chemical, China.

Preparation of Shenfu coal loaded with Ag⁺

The preparation of Shenfu coal loaded with Ag⁺ was carried out by taking 5 g of Shenfu coal and 10 mL of 0.6M AgNO₃ aqueous solution in a beaker containing 90 mL distilled water, and agitated at 100 rpm for the adsorptive equilibrium time using a temperature-controlled shaking water bath. The Shenfu coal (adsorbent) and Ag⁺ solution were separated by filtration and the wet cake of the Shenfu coal was washed several times with distilled water

Correspondence to: Z. Yu (yuzhanjiang2003@126.com).

Contract grant sponsor: Foundation of Shaanxi Educational Committee Shaanxi Province, China; contract grant number: 00JK165.

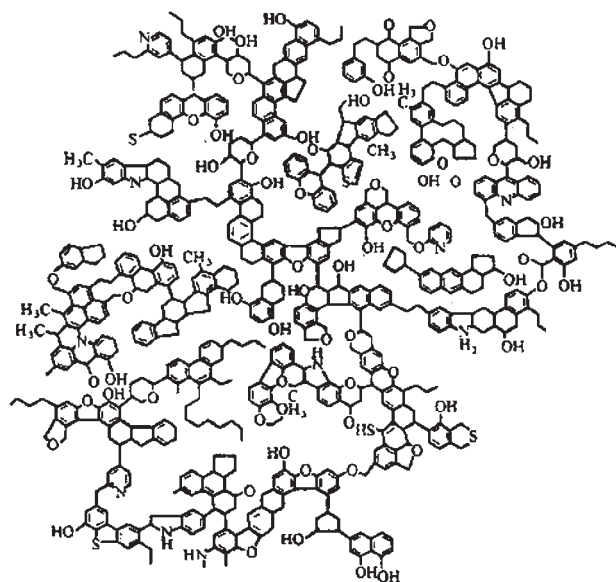


Figure 1 Shinn model of coal molecular structure.¹⁰

till no Ag^+ was detected in solution, and then the wet cake of Shenfu coal loaded with Ag^+ was vacuum dried in an oven at 90°C for 6 h.

Compounding and extrusion

The compounding was performed at 130°C in a high-speed mixer (Yi Tzung Precision Machinery, China, YK-3) at a rotor speed of 60 rpm. The 500 g polymer of LLDPE 7042 was completely softened first for 3 min followed by the addition of coal powder with or without Ag^+ , and the mixing was resumed further till the attainment of a steady torque. The total mixing time was 10 min. Various samples of ACCPE containing Ag^+ of 0.0118, 0.0236, 0.0472, 0.1180, and 0.2360 wt %, and the samples of coal/LLDPE composite with coal content of 0.44, 6.67, 10, 15, and 20 wt % were made, respectively.

Each of the samples of ACCPE or coal/LLDPE composite was put into the hopper of a corotating twin-screw extruder (Nanjing rubber and plastics machinery plant, China, SJS-30) with the screw speeds of 60 rpm and barrel temperature of 240°C , and the thread-like composite extruded by the extruder was cooled down in a water flume and then cut into columned granules by a cutter.

Compression molding

Specimens for elongation tests (based on China national standard of GB/T 1040-1992) rate of Ag^+ release and antibacterial experiments (based on China enterprise standard of QB/T 2591-2003) were compression-molded using a platen vulcanizing press (self-made) at a temperature of 240°C and a pressure

of 20 MPa, and cooled down at ambient temperature for 6 min before being taken out from the mold.

Measurement of mechanical properties

According to China national standard of GB/T 1040-1992, the tensile strength, yield strength, and elongation at break of ACCPE specimens with dumbbell shape were determined using a universal electronic tensile testing machine (Shen Zhen Kai Qiang Li Electronic Company, China, WD-5) at a crosshead speed of 100 mm/min.

Rheology

Rheology measurements of ACCPE with coal powder content of 15 wt % and Ag^+ content of 0.0236 wt % were conducted on a capillary rheometer (Science and Education Apparatus Factory of Jilin University, China, YZL-II) at constant temperature of 220°C , and various shear stresses of 0.125, 0.1875, 0.25, 0.625, 0.75, and 1.25 kg f/cm², and at constant shear stress of 0.625 kg f/cm², different temperatures of 160, 190, 220, and 250°C , respectively.

Immersion test and rate of Ag^+ release

The plate specimens (10 g, 20 mm \times 50 mm \times 1.2 mm) of ACCPE were stored in a cone-shaped flask containing 150 mL aqueous medium (145 mL distilled water + 5 mL 0.1N HNO_3) at temperature of 25°C . HNO_3 was added to prevent the released Ag^+ ions from being metallic silver. The released Ag^+ concentrations in aqueous medium at various immersion times (2, 4, 7, 10, 14, and 20 days) were measured in an atomic absorption spectrophotometer (Solaar M6, USA) with detecting wavelength of 328.1 nm, band pass of 0.5 nm, and burner height of 7.0 mm.

Determination of antibacterial properties

According to China enterprise standard of QB/T 2591-2003 (Test for Antimicrobial Activity and Efficacy), which is similar to USA standard of NEQ and ASTM G21-96 (Standard Practice for Determining Resistance of Synthetic Polymeric Materials to Fungi,

TABLE I
Proximate and Ultimate Analysis of Shenfu Coal

	Proximate analysis (wt %)			Ultimate analysis (wt %)				
	M_{ad}	Ash	V_{daf}	C	H	N	S	O
Shenfu coal	7.29	4.27	36.42	81.75	4.79	1.10	0.38	11.98

M_{ad} , Ash, and V_{daf} respectively represent moisture, Ash, and volatile in coal.

NEQ), the antibacterial test of plate specimens (50 mm × 50 mm × 1.2 mm) against *E. coli* were evaluated by the plate-counting method at Guangdong Detection Center of Microbiology, Guangzhou, People's Republic of China. The plate specimens were first washed many times using 70% ethanol to kill bacteria on the surface. After drying, a 0.3 mL solution of bacteria ((5.0–10.0) × 10⁵ cfu/mL) was added, and the surface was covered by a PE film (50 mm × 50 mm). At a relative humidity of over 90% and temperature of 37 ± 1°C, the samples were incubated for 24 h. Then, they were completely washed with 30 mL of a 1% NaCl solution containing some Tween 80 with pH value of 7.0 ± 0.2, and the active bacteria remained were counted, and the degree of antibacterial or antibacterial effect was calculated using the following equation of R (%) = $(A - B)/A \times 100\%$, where R is the percentage reduction ratio or antibacterial effect (%), A the mean number of bacteria on the blank or control specimens (cfu/specimen), and B the mean number of bacteria on the specimens having antibacterial activity (cfu/specimen).

Infrared spectroscopy and X-ray diffraction

The IR spectra of ACCPE and coal/LLDPE composite without Ag⁺ were obtained at room temperature by means of the FTIR Nicolet Magna IRTM 550 spectrometer (Nicolet Instruments, Madison, WI, USA) at an interval of frequencies 4000–400 cm⁻¹. Frozen and ground samples (1.5 mg) were vacuum-dried at 55°C for 24 h, and then mixed with 75 mg of KBr and compressed into pellets. To obtain the IR spectra, 32 scans were collected.

X-ray pattern of the ACCPE plate (15 mm × 30 mm × 1.2 mm) was obtained on a wide-angle goniometer (D/Max-3c, Rigaku, Japan) with a Cu K α ($\lambda = 0.154$ nm) source. When the the ACCPE sample was tested using goniometer, it had 35 KV working voltage, 50 mA working current, and 1°/min scanning speed.

SEM images

The morphology of crosssection profile of ACCPE plate was characterized by a scanning electron microscopy (JSM-6460, JEOL, Japan) operated at 20.0 kV. The plate sample was fractured by quenching in liquid nitrogen, and then sputter-coated with gold prior to SEM examination.

RESULTS AND DISCUSSION

Elongation tests

The active functional groups (OH, COOH, etc.) and aliphatic chains in coal may react to LLDPE free rad-

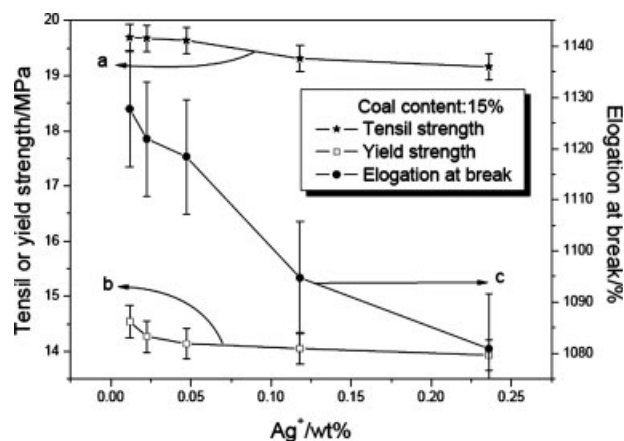


Figure 2 Curves of ACCPE composite's mechanical strength versus Ag⁺ content.

icals produced by shear stress and thermal oxidation¹¹ during extrusion and compression molded, and form crosslinked network structures between coal macromolecule chains and LLDPE macromolecular chains. In Figure 2(c), by and large, the elongation ratio at break of specimen shows gradually decreasing tendency with the increasing Ag⁺ content (in the range of Ag⁺ content explored) because of the decrement of hydroxyl (—OH) active functional groups (silver ions are adsorbed onto hydroxyl oxygen atoms and exchanged with hydrogen atoms¹²), which weaken the interaction between coal and LLDPE macromolecule chains in composite. On the other hand, the decreasing elongation ratio at break of the specimen would attribute to the addition of Ag⁺ into coal, which results in an enhancement of the coal polarity and reduces the compatibility between the polar coal and nonpolar LLDPE interfaces, according to the principles of similitude and compatibility of molecules.¹³

Whereas the tensile strength [seeing Fig. 2(a)] and yield strength [seeing Fig. 2(b)] change less in the range of Ag⁺ loading from 0.0118 to 0.236 wt %, which demonstrate that the very small changing of Ag⁺ loading affects the tensile or yield strength inconspicuously. In other words, the tensile or yield strength is not sensitive to Ag⁺ loading studied in our concerning range except the elongation ratio at break. This is favorable for the preparation of ACCPE composite in application of engineering.

Rheology

For investigating the process property of ACCPE, the rheological properties are performed on the capillary rheometer. The non-Newtonian index, n , is obtained using eq. (1), the apparent viscosity, η , is

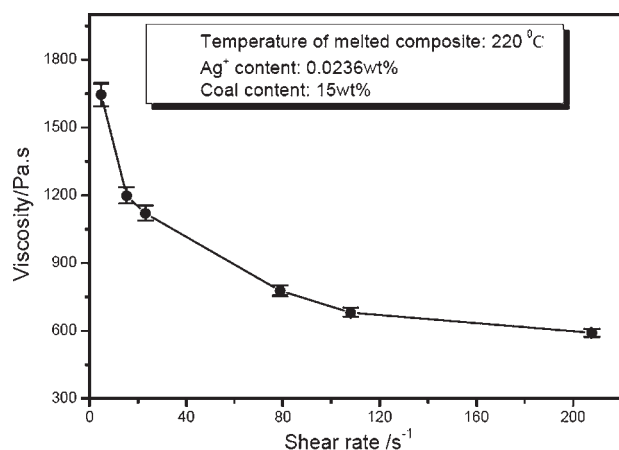


Figure 3 Curve of melt flow: viscosity versus shear rate.

calculated using eq. (2), and the viscous flow activation energy is obtained using Arrhenius eq. (3).

$$\tau = K\dot{\gamma}^n, \quad (1)$$

$$\eta = \tau/\dot{\gamma}, \quad (2)$$

$$\eta = Ae^{E_\eta/RT}, \quad (3)$$

where τ is the shear stress (kgf/cm^2), $\dot{\gamma}$ shear rate (s^{-1}), η apparent viscosity (Pa s), and E_η viscous flow activation energy (kJ/mol).

Figure 3 represents curve of melt flow of the ACCPE at a constant temperature 220°C and various shear stresses of 0.125, 0.1875, 0.25, 0.625, 0.75, and $1.25 \text{ kg f}/\text{cm}^2$. The viscosity of melted composite decreases with the increasing of shear rate and tends to nearly constant value, which demonstrates that the viscosity is sensitive to shear rate and the melted composite is of pseudoplastic fluid. Furthermore, the non-Newtonian index n of $0.68197 < 1$ (as listed in Table II) also supports the above-mentioned conclusions, and this Shear thinning flow behavior would benefit the processability.

Figure 4 shows curve of viscosity as a function of melted temperature of the ACCPE at a constant shear stress of $0.625 \text{ kg f}/\text{cm}^2$ and various melted temperatures of 160, 190, 220, and 250°C . The viscosity of melted composite depends on the variation of temperature and decreases with the increasing of temperature, finally tends to nearly constant value, which reveals that the viscosity of melted composite is sensitive to temperature and the melted composite is of pseudoplastic fluid. Moreover, the non-Newtonian index n of $0.30729 (< 1)$, listed in Table II) also proves the validity of the above-mentioned explanations, and these temperature-sensitive, shear thinning flow behavior, and the lower viscous flow activation energy E_η of $20.84 \text{ kJ}/\text{mol}$ (calculated in Table II) show that the ACCPE composite would feature a high processability during the process of extrusion.

Morphology of ACCPE

The crosssection-profile SEM images of ACCPE are presented in Figure 5. It is observed that the coal particles exhibit fine dispersion in LLDPE matrix and possess compatibility with LLDPE macromolecule chains to some extent due to the aliphatic chains in coal, having definite similitude and compatibility with macromolecules in LLDPE. Hence, the ACCPE holds adequate mechanical properties when compared with that of pure LLDPE resin.

Infrared spectroscopy and XRD pattern

In Figure 6, the infrared spectra on ACCPE and coal/LLDPE composite exhibit bands at 3396.76 and 1098 as well as 3369.51 and 1090 cm^{-1} , respectively. The bands at 3396.76 and 3369.51 cm^{-1} correspond to hydroxyl $-\text{OH}$ vibrations, and the bands at 1098 and 1090 cm^{-1} attribute to ether bond vibrations, while band ranges from 1437.41 to 1180.07 cm^{-1} is ascribed to $\text{C}-\text{H}$ bending vibration of cyclane and

TABLE II
Viscous Flow Activation Energy and Non-Newtonian Indexes of ACCPE at Various Conditions

Melted temperature ($^\circ\text{C}$)	Shear rate (s^{-1})	Non-Newtonian index n	Activation energy E_η (kJ/mol)	
220	7.37	0.68197	Blank	
	15.34			
	17.44			
	78.86			
	108.05			
	207.76			
160	38.22	0.30729	20.84	
	190			72.20
	220			110.42
	250			164.57

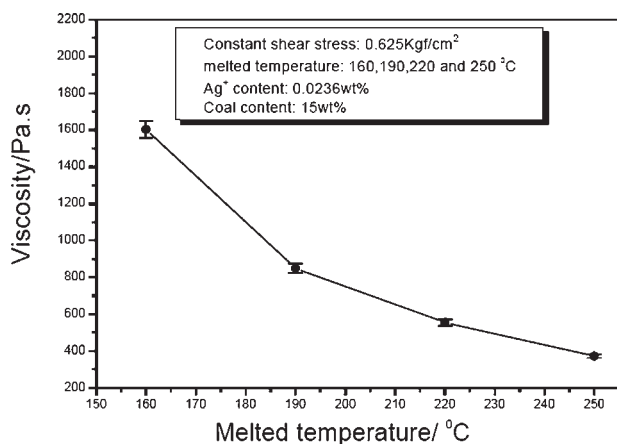


Figure 4 Curve of viscosity as a function of melted temperature.

fat hydrocarbon, methylene $-\text{CH}_2$ bending vibration, alcohol hydroxy $\text{C}-\text{O}$ stretching vibration, and residue $-\text{NO}_3$ vibration, respectively. After adsorbing Ag^+ , the intensity of hydroxy $-\text{OH}$ and ether bond vibrations has weakened intensively and the peak of hydroxy vibrations produces red shift from 3396.76 to 3369.51 cm^{-1} and the peak of ether bond vibrations shifts from 1098 to 1090 cm^{-1} , which indicates that the most of silver ions has adsorbed on oxygen atom of hydroxy $-\text{OH}$ and exchanged it with hydrogen atom, and a small part of silver ions has adsorbed onto ether bond oxygen atoms. In addition, as a result of Ag^+ adsorption of oxygen atom, the peak intensity of hydroxy $\text{C}-\text{O}$ (at a band 1180.07 cm^{-1}) stretching vibration and the methylene $-\text{CH}_2$ (1318.22 cm^{-1}) bending vibration has intensified obviously and produced red shift. Whereas the peak intensity of $\text{C}-\text{H}$ (1437.41 cm^{-1}) plane bending vibration has weakened slightly. The peak at a band 1383.91 cm^{-1} is ascribed to the residue $-\text{NO}_3$ obtained from AgNO_3 solution.

The XRD pattern of ACCPE shows that there appears to be no obvious peaks of the silver crystal structure when compared with the XRD pattern of the pure silver powder as shown in Figure 7, which

further indicates that the Ag^+ has adsorbed onto hydroxy oxygen and ether oxygen (chemiadsorption) instead of existing in metallic silver. The peaks of the XRD pattern at 21.44° , 23.78° , and 36.14° are corresponded to various LLDPE crystal planes diffraction and the rest are nearly attributed to minerals in coal such as pyrite, quartz, sphalerite, etc. Silver ions show considerable superiority over the metallic silver against bacteria. Yoshihiro and Yasushi¹⁴ investigated the relationship between the oxidation state of silver and antibacterial activity by the electrochemical method, and they observed no antibacterial activity when the oxidation state of silver was changed from $+1$ to 0 . Hence, the data from XRD show that no metallic silver lattice peaks are detected and the silver in Shenfu coal exists in Ag^+ form, which supports the higher antibacterial activity of ACCPE against *E. coli* (Fig. 8).

Antibacterial properties

The antibacterial activity against *E. coli* was investigated, and the results are illustrated in Figure 8. It can be seen that both ACCPE and coal/LLDPE without Ag^+ antibacterial composites exhibit strong antibacterial activity against *E. coli*. The *E. coli* removal of the coal/LLDPE composite increases with increasing coal content and reaches maximum (99.08%) while the coal content is 15 wt %, which then rapidly decreases to 58.44% with the coal content of 20 wt %. This can be explained that with increasing the coal content from 15 to 20%, the proportion of organic nitrogen and carbon source in composite needed for *E. coli* metabolism increases. This increase of organic nitrogen and carbon source promotes the *E. coli* propagation and growth,⁹ and weakens the coal/LLDPE composite's antibacterial effect, so that the antibacterial activity of coal/LLDPE containing 20% coal decreases when compared with that of coal/LLDPE containing 15% coal. Yet, by adding Ag^+ content of 0.0236 wt %, the *E. coli* removal of the ACCPE has been enhanced up to 99.91% while the coal content is of 15 wt %.



Figure 5 SEM images of ACCPE.

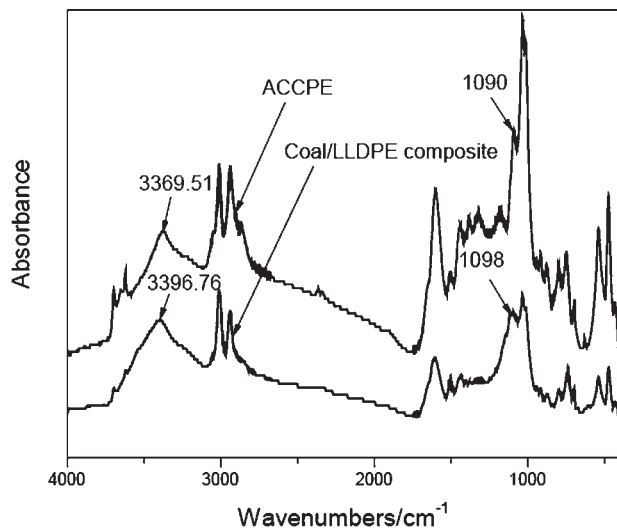


Figure 6 Infrared spectra of ACCPE and Coal/LLDPE composite.

Qualification of Ag⁺ release

Atomic absorption spectroscopy was used for the quantitative determination of the silver ion concentration in the analyte. Figure 9 shows the concentration of silver ion release (a) and the rate of silver ion release (b) in distilled water medium as a function of immersion time. Figure 9(a) demonstrates that the concentration of released silver ion increases with the increase in immersion time, and the accumulative total of Ag⁺ release gets to 1.1 wt % of total Ag⁺ in composite after 14 days. This tiny Ag⁺ release of 1.1 wt % in total Ag⁺ in composite within 14 days ensures keeping the ACCPE with long-lasting biocide and broad spectrum of antibacterial activity. Figure 9(b), which is a derivative curve of Figure 9(a), shows clearly the rate of Ag⁺ release for the ACCPE upon contact with water. It is seen that after an initial increase, the rate of Ag⁺ release reaches a minimum near the seventh day. Reversely, the rate

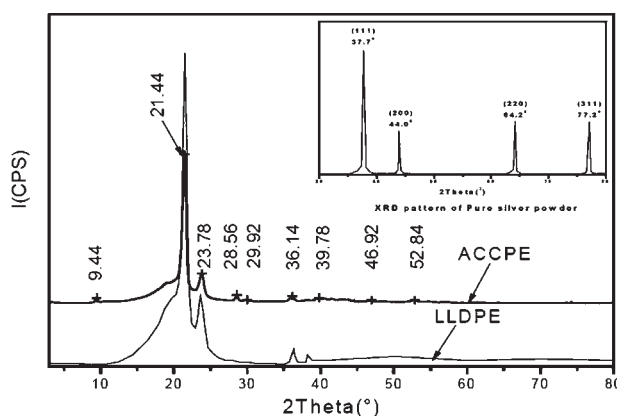


Figure 7 XRD patterns of ACCPE and LLDPE.

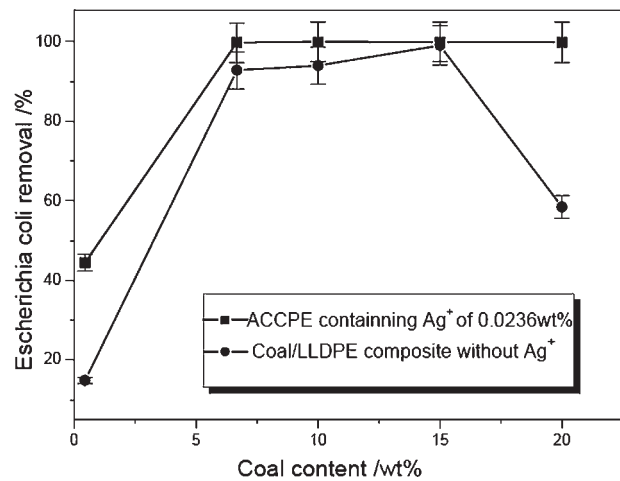


Figure 8 Antibacterial tests of composites.

of Ag⁺ release increases after the 7th day and finally tends to a plateau after the 10th day, which can be explained as follows: (a) The initial release of silver ions (between day 2 and 4) must be from those silver ions, which are encapsulated within the surface layers of the specimen with instantaneous migration into water medium⁸; (b) For the subsequently slow release of Ag⁺ from the interior part of the specimen, water has to cross or overcome the diffusion barrier such as the porous-like or “free volume” microcracks between the macromolecule chains of the ACCPE^{8,15,16}; (c) The abrupt rise with the rate of Ag⁺ release (after the seventh day) is because of the percolation, plasticization, and wet swelling of water,^{15–17} which could provide substantial mobility to the coal macromolecular chains and facilitate the rate of Ag⁺ release and migration. So, we believe that Ag⁺ release will be influenced by the equilibrium swelling characteristics of the coal component in ACCPE.⁸

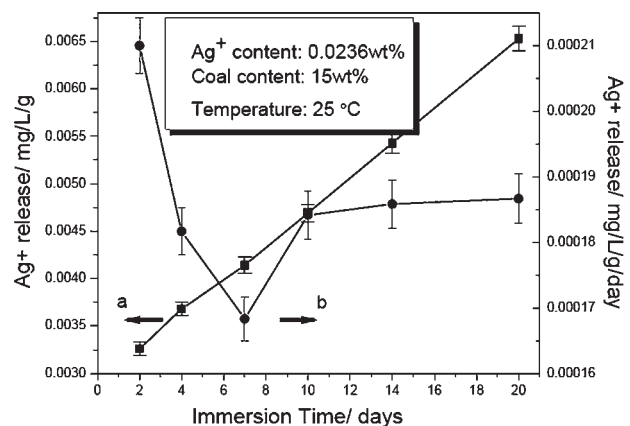


Figure 9 Ag⁺ release as a function of time (a), and rate of Ag⁺ release from the ACCPE (b).

CONCLUSIONS

By analysis of mechanical, rheological, Ag⁺-releasing, and antibacterial properties of ACCPE antibacterial composite, we conclude that the composite shows favorable mechanical properties, features a higher processability, and exhibits a strong antibacterial activity against *E. coli*. The Ag⁺ in composite is of steady release after the 10th day immersion in aqueous medium. The coal and silver ion in the composite possess superimposed effect on antibacterial activity against *E. coli*. The IR and XRD pattern show that most of silver ions adsorbed onto hydroxy oxygen atoms and exchanged with hydrogen atoms, a small part of silver ions adsorbed onto ether bond oxygen atoms.

References

1. Zhao, G.; Stevens, E. *Biomaterials* 1998, 19, 27.
2. Fu-Ren, F.; Bard, A. *J Phys Chem B* 2002, 106, 279.
3. Demling, R.; de Sant, L. *Wounds* 2001, 13, 11.
4. Uchida, M. *Chem Ind* 1995, 46, 48.
5. Grier, N. In *Silver and Its Compounds in Disinfection, Sterilisation and Preservation*; Block, S. S., Ed.; Lea and Febiger: Philadelphia, 1983; p 375.
6. Kusnestov, J.; Elomaa, N.; Martikainen, P. *Water Res* 2001, 35, 4127.
7. Keheler, J.; Bashant, J.; Johnson, L.; Li, Y. *World J Microbiol Biotechnol* 2002, 18, 133.
8. Kumar, R.; Münstedt, H. *Biomaterials* 2005, 26, 2081.
9. Anirban, G.; Malay, C. *Water Res* 1995, 29, 511.
10. Shinn, J. H. *Fuel* 1984, 63, 1187.
11. Zhizhen, J.; Yunming, L.; Dingyu, X.; Shushen, X. *Polymer Chemistry and Physics, China Light Industry: Beijing*, 1981; p 382.
12. Zhanjiang, Y.; Anning, Z.; Jianlin, Q.; Tianjun, Z. *Microporous Mesoporous Mater* 2005, 85, 104.
13. Zhou, A.; Shucai, G., et al. *J China Coal Soc* 1998, 23.
14. Yoshihiro, I.; Yasushi, K. *J Inorg Biochem* 1997, 67, 377.
15. Murthy, N. S.; Stamm, M.; Sabilia, J. P.; Krimm, S. *Macromolecules* 1989, 22, 1261.
16. Wang, W.; Sain, M.; Cooper, P. A. *Compos Sci Technol* 2006, 66, 379.
17. Szeliga, J.; Marzec, A. *Fuel* 1983, 62, 1229.